Available online at www.sciencedirect.com

ScienceDirect

Advances in Space Research 61 (2018) 1761–1775

ADVANCES IN SPACE RESEARCH
(a COSPAR publication)

www.elsevier.com/locate/asr

On the occurrence and strength of multi-frequency multi-GNSS Ionospheric Scintillations in Indian sector during declining phase of solar cycle 24

V.K.D. Srinivasu [a], N. Dashora [b,*], D.S.V.V.D. Prasad [a], K. Niranjan [a], S. Gopi Krishna [c]

[a] *Department of Physics, Andhra University, Visakhapatnam 530003, India*
[b] *National Atmospheric Research Laboratory, Gadanki 517 112, India*
[c] *Indian Institute of Geomagnetism, Panvel, Navi Mumbai 412028, India*

Received 31 March 2017; received in revised form 1 August 2017; accepted 30 August 2017
Available online 8 September 2017

Abstract

This study presents unique perspectives of occurrence and strength of low latitude ionospheric scintillations on multiple signals of Global Navigation Satellite System (GNSS) and its frequency dependence using continuous observation records of 780 nights. A robust comparative analysis is performed using scintillation index, S4 and its variation during pre-midnight and post-midnight duration from a GNSS receiver located at Waltair (17.7°N, 83.3°E), India, covering period from July 2014 to August 2016. The results, generally exhibit the impact of declining phase of solar cycle 24 on occurrence and strength of scintillations, which, however, is evidently different over different frequencies transmitted from different GNSS systems. A deeper quantitative analysis uniquely reveals that apart from the solar cycle and seasonal effects, the number of visible satellites of a selected GNSS markedly affect the occurrence and also the strength. Processing scheme of adopting 6 hourly time windows of pre-midnight and post-midnight brought a novel result that the strength and occurrence of strong scintillations decrease with declining solar activity during pre-midnight hours but remarkably increase for moderate and weak scintillations during post-midnight. The physical processes that dominate the post-midnight equatorial ionosphere are invoked to explain such variations that are special during declining solar activity. Finally, inter-GNSS signal analysis in terms of the effect of strong, moderate and weak scintillations is presented with due consideration of number of satellite passes affected and frequency dependence of mean S4. The quantitative results of this study emphasize for the first time effect of low latitude scintillation on GNSS signals in Indian zone under changing background solar and seasonal conditions.

Keywords: Ionospheric irregularities; Morphology of scintillations; Equatorial and low latitude; Solar cycle; Radio wave dispersion; Global navigation satellite system; Multi-frequency scintillations

1. Introduction

The occurrence and strength of post-sunset ionospheric irregularities in the equatorial and low latitude ionosphere have remained a challenging problem for the ionospheric researchers for last many decades. This has been due to the complex interplay of multiple physical processes operative for triggering, growth, drift and decay of large scale ionospheric F region irregularities known as equatorial plasma bubbles (EPBs) (Haerendel, 1973; Woodman and La Hoz, 1976; McClure et al., 1977; Tsunoda, 1980; Tsunoda et al., 1982). It has been well established that several scales of electron density irregularities are produced within an EPB through an electrodynamics assisted turbulent cascade process encompassing from hundreds of km

* Corresponding author.
E-mail address: ndashora@narl.gov.in (N. Dashora).

https://doi.org/10.1016/j.asr.2017.08.036
0273-1177/

scales down to cm scales (Basu and Basu, 1981; Yeh and Liu, 1982; Kelley, 2009). The EPBs pose a serious threat to satellite navigation and communication (Kintner et al., 2001; Carrano and Groves, 2010), specifically for global navigation satellite systems (GNSS). The GNSS have provided a large number of applications in modern society that use trans-ionospheric propagation, specifically, in L-band. GNSS is a generic name of all the satellite constellations primarily aimed at providing navigation and the majority of signals from such satellites fall in L-Band (see Hofmann-Wellenhof et al., 2008, for technical details). Theoretically, the radio wave scattering and diffraction processes in a growing EPB ranging between 300 and 400 m scale sizes (known as Fresnel scale) produce scintillation in L-band (Kintner et al., 2001). The scintillations in equatorial and low latitude, where large vertical electron density gradients exist, produce sudden and strong signal fading, scattering and other effects and thus eventually may lead to loss of signal power (Aarons, 1982). The presence of EPBs in the line of sight between a satellite and receiver produces random perturbations in amplitude and phase besides sharp gradients in total ionospheric delay (or total electron content) (Basu et al., 1999; Dashora and Pandey, 2005). These perturbations cause several hindering effects on GNSS signals like multiple phase cycle slips, loss of lock in phase lock loop in the receiver, loss of navigation data for more than a few minutes causing radio black-out for GNSS receivers (e.g. Wernik et al., 2003; Valladares et al., 2004; Dashora and Pandey, 2005; Rama Rao et al., 2006, 2009; Venkatesh et al.; 2015; Ghafoori and Skone, 2015). Hence, the EPBs become an impediment for all the GNSS applications that require accuracy, continuity, availability and integrity at every time, everywhere (Conker et al., 2003; Carrano et al., 2012; Das Gupta et al., 2004).

Ionospheric scintillations dramatically show varying effect due to dispersion for changing the frequency of transmission, even within L-band as reported in recent studies (Muella et al., 2009; Spogli et al., 2013; Hlubek et al., 2014). As far as the Indian ionospheric region is concerned, it is strongly influenced by the presence of the geomagnetic equator passing right through the southernmost tip of Indian peninsular region. Thus, the complete Indian land mass that utilizes the navigation solutions is prone to the scintillation threats under phenomenon of EPB (Chakraborty et al., 2014). In the aforementioned context, the present study from Indian sector provides recent results from multi-frequency GNSS scintillation analysis. This paper presents occurrence of scintillation, its strength, dependence on availability of satellites in a GNSS system and the variability during descending solar activity period of cycle 24 from 2014 to 2016. The following sections present the observations, comparative analyses and conclusions from this study.

2. Data and observations

The data, observations and all the results are briefly mentioned in this section. The aim of this section is to give an overview of results so that a comparative analysis with cross referencing of results is possible in a later section. Continuous GNSS observations have been made at Waltair (17.7°N, 83.3°E, Geomag. Lat. 8.71°N), a low latitude station in the Indian sector using a Novatel make multi frequency GNSS receiver known as GPStation-6 GISTM (GNSS Ionospheric Scintillations and TEC Monitor) for a period of 26 months from 01 July 2014 to 31 August-2016. This period marks the presence of descending phase of the solar cycle 24. GISTM records the raw amplitude and phase measurements of the satellite signals at different frequencies from various systems of GNSS at a sampling rate of 50 Hz. This receiver is capable of measuring signals from satellites of GPS (Global Positioning System), GLONASS (GLObal NAvigation Satellite System), Galileo and Indian SBAS (Space Based Augmentation System) called GAGAN (GPS aided geo augmented navigation). A data parsing utility computes the ISMR (ionospheric scintillation measurement record) parameters such as amplitude scintillation index S4, phase scintillation index (Sigma-Phi) and other parameters of ionospheric interest at one minute interval. The GISTM do not record scintillation data over L2 frequency of GPS because of excess noise due to semi-codeless tracking of P (Y) code (see user manual of GPStation-6, 2012).

Table 1 provides the details of L-band frequencies of different systems and Table 2 provides the duration of data records which are utilized in this study that include L1 and L5 frequencies of GPS, L1 and L2 bands of GLONASS, E1, E5A, E5B and E5AltBOC frequencies of Galileo and L1 frequency of SBAS-GAGAN (on PRNs 127 and 128). The amplitude scintillation index (S4) (Briggs and Parkins, 1963; Dashora and Pandey, 2005) recorded internally at sample rate of 50 Hz in the receiver and computed every minute on the minute in the PC is used in this study. The amplitude of GNSS signal is affected by multi-path at the antenna due to the interference from reflected signals

Table 1
The signals transmitted by different GNSS systems, corresponding frequencies, wavelengths and the Fresnel scales of ionospheric irregularities.

GNSS system	GPS		GLONASS		Galileo				Indian SBAS
	L1CA	L5Q	L1CA	L2P	E1	E5A	E5B	AltBOC	L1CA
Frequency (MHz)	1575.42	1176.5	1593–1609	1238–1254	1575.42	1176.45	1207.14	1191.79	1575.42
Wavelength (m)	0.190	0.255	0.188–0.186	0.242–0.239	0.190	0.255	0.248	0.251	0.190
Fresnel scale $\rho = \sqrt{2\lambda z}$ (m)	365	422	363–361	412–409	365	422	417	419	365

from close by structures at lower elevations angles. To avoid the site-specific multipath, generally an elevation cut-off is used. The cut-off angle can be chosen based on the altitude of the antenna and the site-specific structures spread around. For this site, although the antenna is mounted on roof-top of building, a cut-off angle of 30 degree is found satisfactory to reject multipath effects. Also, to further reduce the effect of ambient, thermal and electronic noise from S4 index, only the data with $S4 > 0.17$ (corresponding to $SNR > 3$ dB) are considered for further analysis. This limit has been obtained from the S4 observations on nights without ionospheric scintillation events. It shall be noted that GPS transmits L5 frequency only over 10 out of 31 active satellites whereas each satellite of GLONASS transmits different frequency selected from a band spread around central frequencies at 1602 MHz and 1246 MHz. All the results presented in this work pertain to nocturnal variations in S4 vis-à-vis the frequency of signals and the magnitude of S4 along the occurrence statistics and availability. Following a similar approach as Akala et al. (2016), Fig. 1a and b present per minute maximum S4 among the visible satellite PRNs under the above mentioned thresholds and criteria. The computed S4 during the time span 18:00–06:00 IST (Indian Standard Time = UT + 05:30 h) for the period of observations is presented as color scale in Fig. 1a. The color bar shows the strength of S4 index in 3 categories namely weak ($0.17 < S4 \leq 0.3$ i.e. 3–6 dB), moderate ($0.3 < S4 \leq 0.45$ i.e. 6–10 dB) and strong ($S4 > 0.45$ i.e. 10 dB) scintillations following the relationship developed over time by Whitney (1974), Secan et al. (1995) and Rama Rao et al. (2006). The gray background of Fig. 1a and b represents no scintillation on a given night unless specifically marked for no observations. The variations of weighted proxy index of F10.7 cm solar flux (Dashora and Suresh, 2015) is given on the top axis of the first column in Fig. 1a and 1 b (curve in magenta color) to highlight the descending trend in the solar activity in the concerned period. A visual inspection of different columns in both the figures provide a direct evidence of existing similarities and differences in occurrence of peak S4 per minute among different frequencies and also among different GNSS constellations. One interesting aspect highlighted in the first and second columns is that per minute peak S4 index shows the well-known seasonal pattern of low latitudes with higher (lower) values in equinoxes (solstices), similar to the results from previous studies like Tsunoda (1985), Rama Rao et al. (2006), Muella et al. (2009) and Abadi et al.(2014). It is obvious that the occurrence and the intensity of S4 are largely different among various constellations and signals. Although, the temporal width of occurrence of scintillation on a given night is found maximum for GPS L1 signal, it must be noted that the number of visible satellites from a given constellation on a given night was also maximum for GPS. Otsuka et al. (2006) and Abadi et al. (2014) have discussed the effect of geometry and patterns in the drift of EPBs in pre-mid-night sector on the GPS scintillation in detail. Thus, in light of these studies, the results from the present study suggest that it is quite possible that the zonally drifting EPBs in pre-midnight sector provide more probability of crossing the line of sight of GNSS signals when more satellites are visible over a site from a particular constellation. However, it shall be noted that the availability of satellites remain the same from one night to another for a given constellation but the dynamics as well as zonal and latitudinal extent of the EPBs vary in same time window and volume of space.

Thus, the results in Fig. 1a and b indicate a necessity to quantify the occurrence and the strength of S4 vis-à-vis the visibility of satellites and the frequency of GNSS signals, which has not been emphasized clearly in earlier studies. Hence, to accomplish this task, the nocturnal data is segregated into two time windows namely pre-midnight during 18:00–00:00 IST and post-midnight during 00:00–06:00 IST. Notably, the spatial ionospheric coverage above elevation angle of 30° provides a horizontal latitude-longitude grid of about $5° \times 5°$ at an altitude of about 350 km over Waltair. Thus, the choice of the 6 h window and selection of per minute peak S4 from any of the visible satellites in this time window facilitate the spatio-temporal extent of scintillation within this volume. Fig. 2a and b respectively present the peak S4 from all the visible satellites from 6 hourly pre-midnight and post-midnight time windows as observed from different constellations for all the signals in respective panels. To further look into the number of satellites affected by scintillation compared to the total visible satellites, the total number of satellite passes (shown as green bars) and the number of satellite passes having scintillations (shown as red bars) are given in Fig. 3a and b, respectively for the two time windows. The seasonal occurrence has been obtained by binning the monthly percentage occurrence of scintillations. Scintillation occurrence is defined when S4 is higher than 0.17 for continuous 5 min for any satellite for a given constellation during a night. The results for monthly percentage occurrence are presented in Fig. 4a and b, respectively for pre-midnight and post-midnight windows. Finally, the scintillation observations are segregated into weak ($0.17 < S4 < 0.3$ i.e. 3–6 dB), moderate ($0.3 < S4 < 0.45$ i.e. 6–10 dB) and strong ($S4 > 0.45$ i.e. more than 10 dB) scintillations in terms of affected number of satellite passes. The results of this segregation are presented in Fig. 5a and b respectively for pre-midnight and post-midnight windows, wherein each columnar panel shows the monthly occurrence of scintillation in terms of total number of affected passes of satellites in each of the category of scintillation, respectively shaded by blue (weak), green (moderate) and red (strong) colors. The frequency dependence of mean S4 is also computed resulting into prominent slopes for different constellations as given in Fig. 6a. It is interesting to note the difference of slope among GPS, GLONASS and Galileo signals and the statistics of the difference in magnitude of mean S4 for different frequencies in GPS and GLONASS (Fig. 6b).

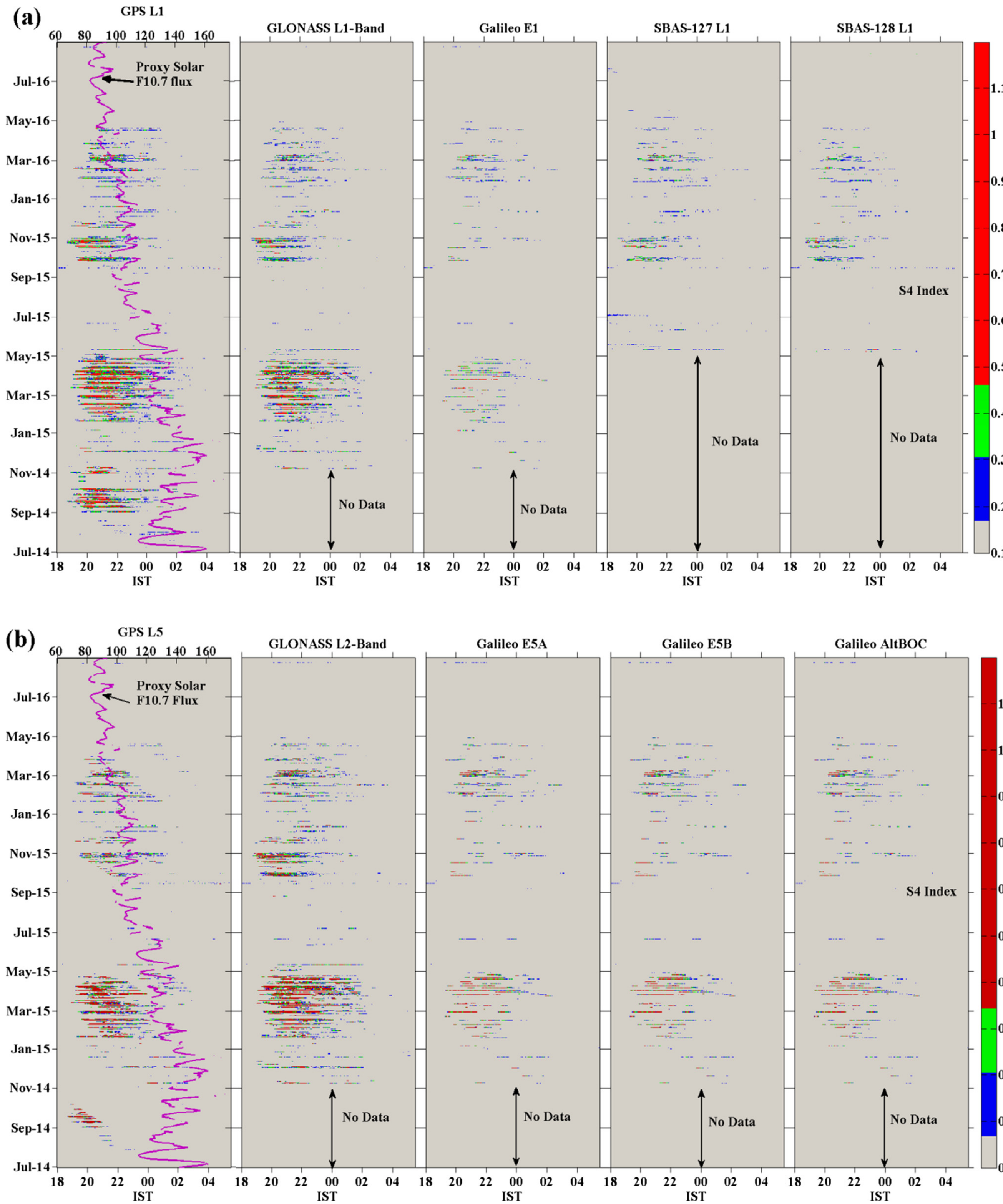

Fig. 1. (a) Top panels show the variations of per minute peak S4 for signals in L1-band from various systems (column-wise) from July 2014 to August 2016. Variations in Proxy Index for F10.7 cm solar EUV flux is shown in first left column by magenta color. (b) Same as (a) but for signals in L2 and L5-bands. The gray background color shows no scintillation as per the criteria chosen in this study. No data record is shown by vertical arrow in respective panels. It shall be noted that the observation geometry of SBAS is fixed compared to all other constellations. (For interpretation of the references to color in this figure legend, the reader is referred to the web version of this article.)

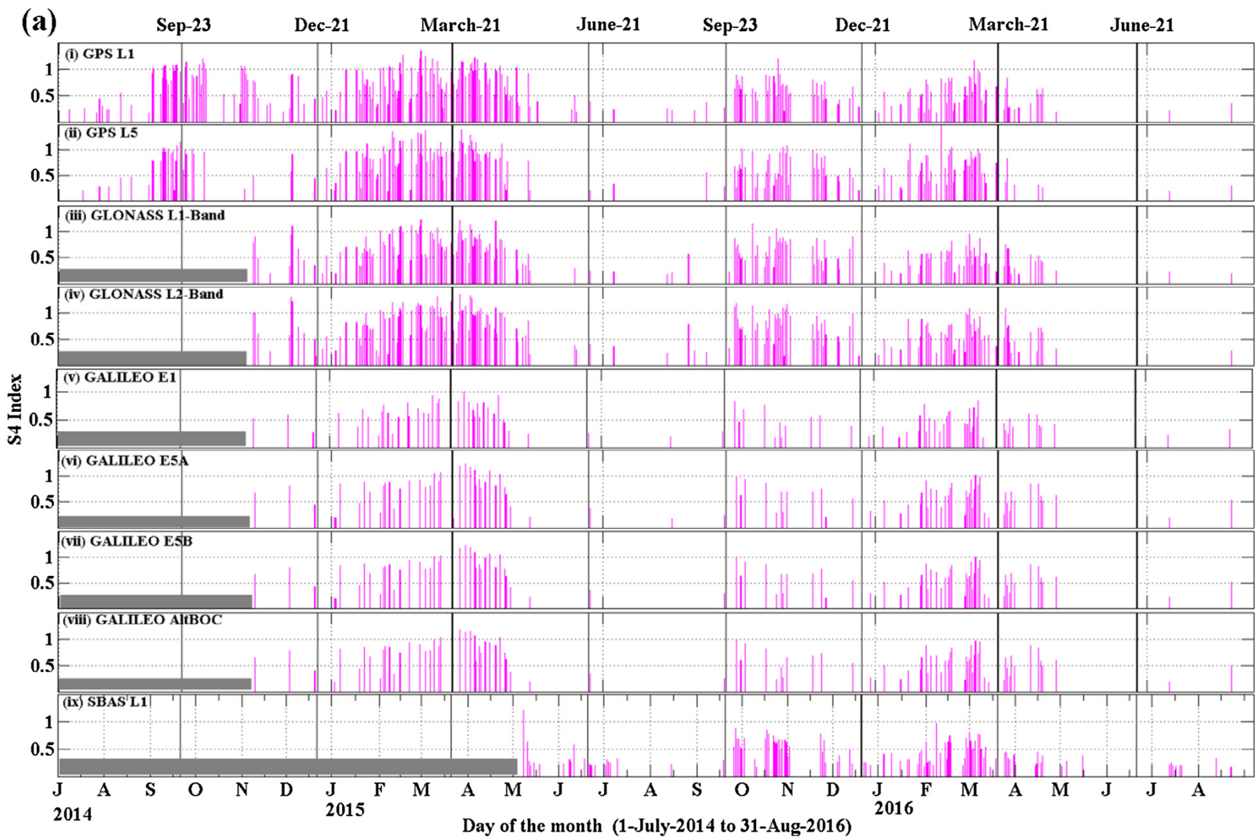

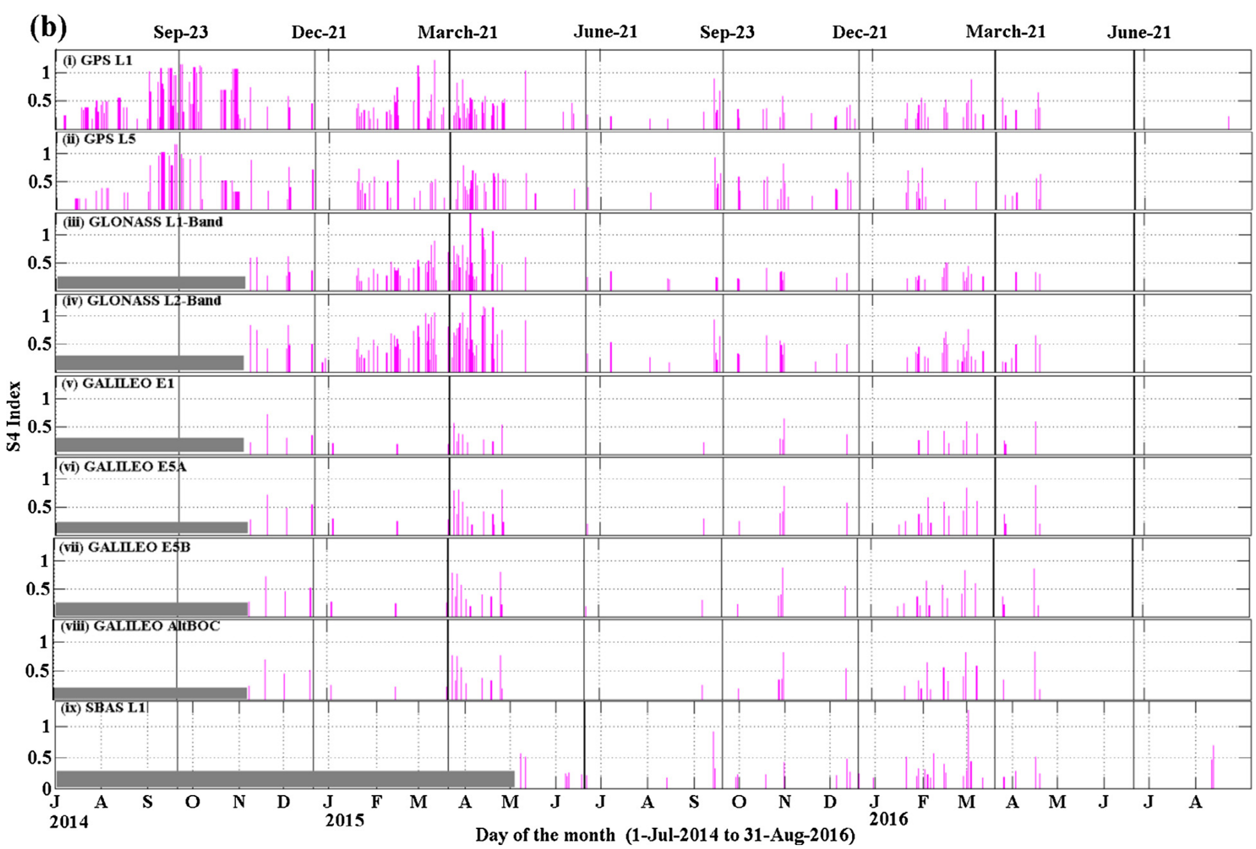

Fig. 2. Value of peak S4 on each night from all the visible satellites in 6 hourly (a) pre-midnight and (b) post-midnight time windows as observed from different constellations for all the GNSS signals in L1, L2 and L5-bands. The horizontal gray bars along abscissa in different panels show period of no data record for that particular frequency. The bottom panel shows all the nights from 1 July 2014 to 31 August 2016 and the top panel indicates the nights of respective equinoxes and solstices.

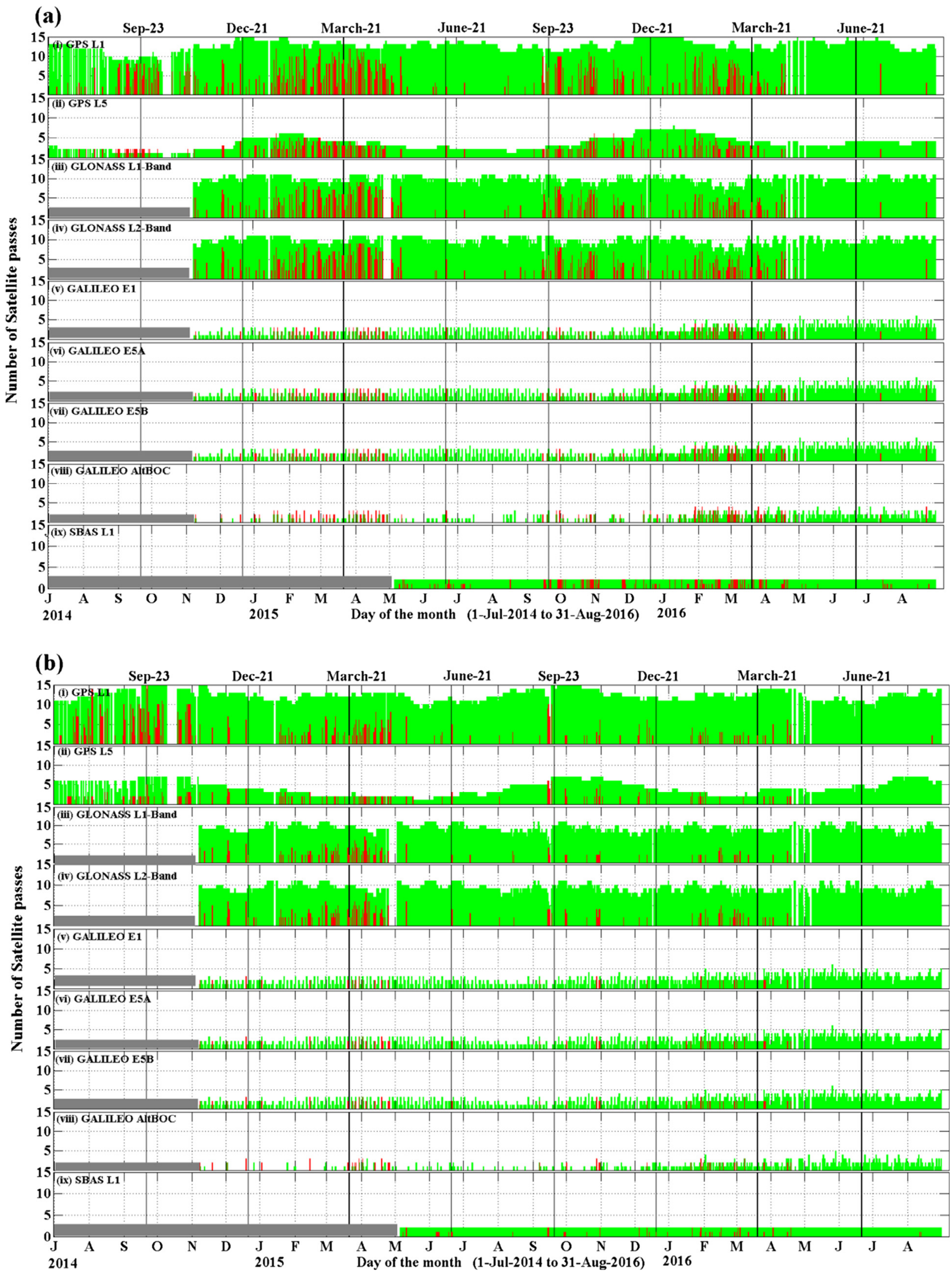

Fig. 3. Number of satellite passes within 6 hourly duration affected by scintillation (red bars) versus the total number of satellite passes (green bars) on a night for all the GNSS signals respectively in (a) top panels for pre-midnight and (b) bottom panels for post-midnight time windows. Nights are shown on bottom panels and no data records are shown by horizontal gray bars for the respective durations and frequency. (For interpretation of the references to color in this figure legend, the reader is referred to the web version of this article.)

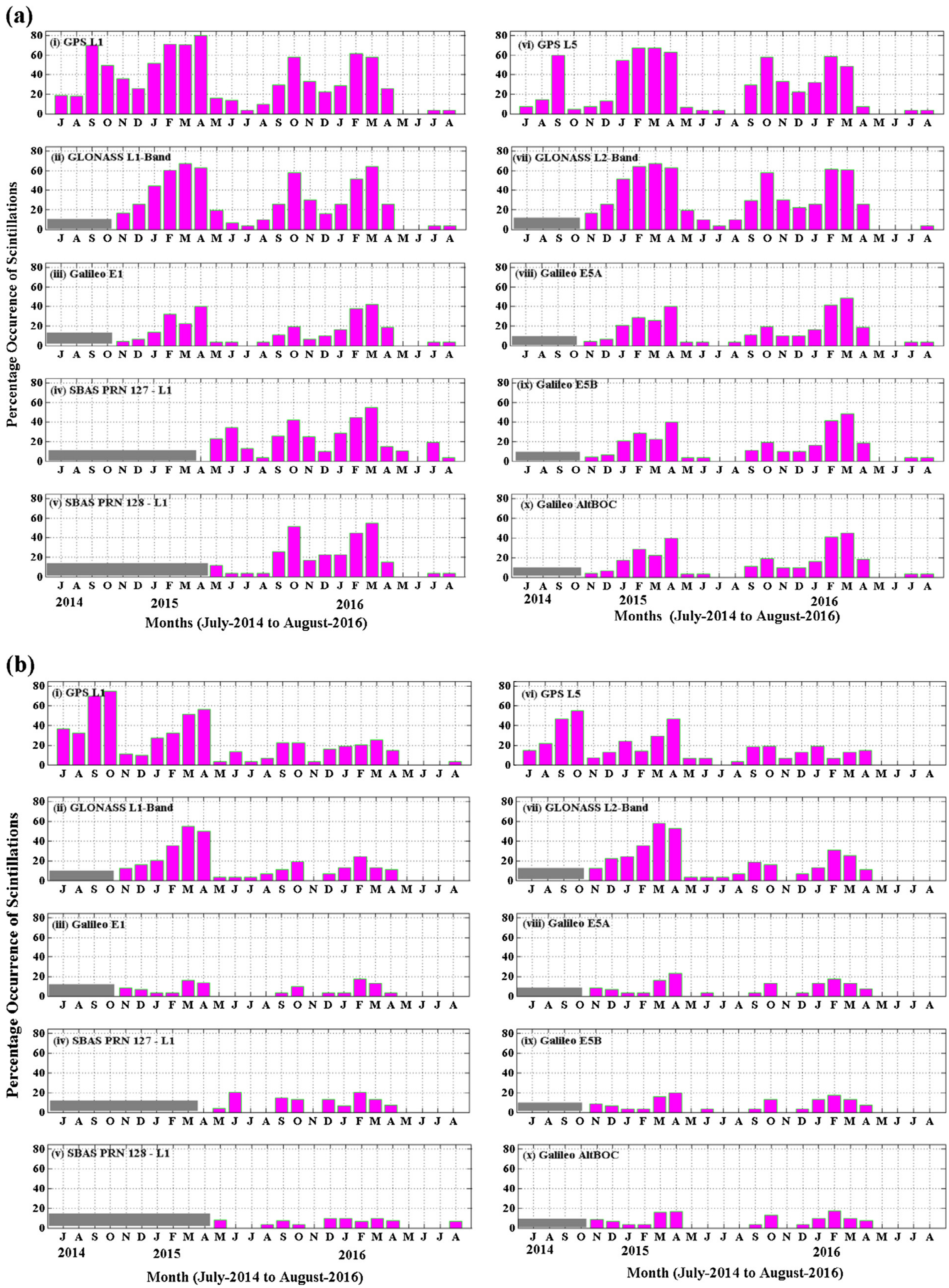

Fig. 4. Monthly percentage occurrence of scintillation shown by magenta bars for all the GNSS signals respectively in (a) top panel for pre-midnight and (b) bottom panel for post-midnight time windows. No data record is shown by horizontal gray bars for the respective durations and frequency. (For interpretation of the references to color in this figure legend, the reader is referred to the web version of this article.)

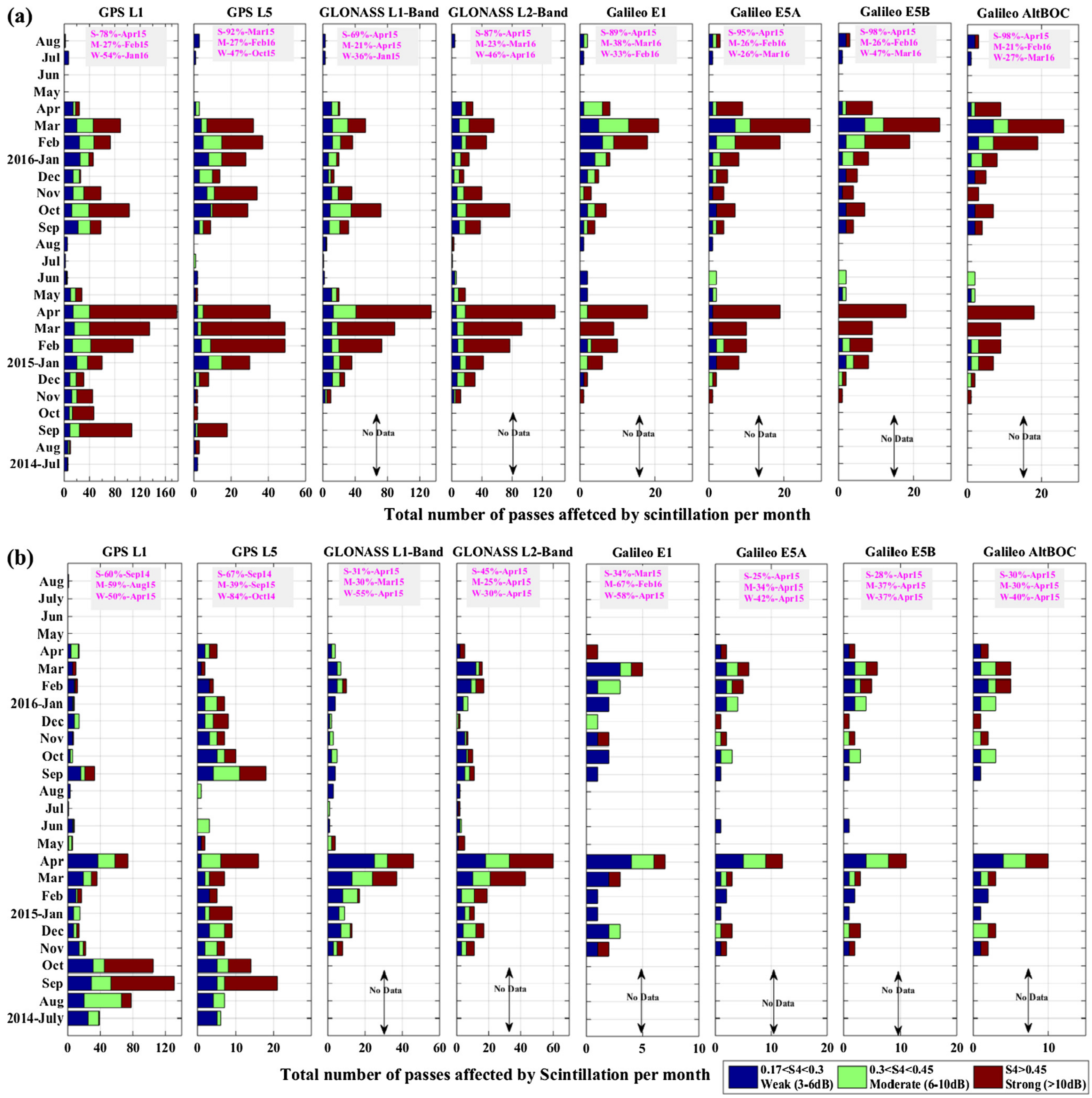

Fig. 5. The abscissa of the columnar panels show the total number of satellite passes affected by scintillations in weak (blue), moderate (green) and strong (red) for a given month and the ordinate show the month of the year, respectively in (a) top panels for pre-midnight and (b) bottom panel for post-midnight time windows. Note that each panel is shown in different range for abscissa to clearly describe the statistics for different GNSS signals. On top of each panel, the highest percentage occurrence of affected satellite passes for each category in a specific month is given as text annotation. Specific month corresponding to the highest percentage occurrence is indicated by S-Strong, M-moderate and W-weak symbol. No data record is shown by vertical arrow in respective panels. (For interpretation of the references to color in this figure legend, the reader is referred to the web version of this article.)

3. Comparative analysis of occurrence and strength of GNSS amplitude scintillations

The summative description of the observations as given in Section 2 above provides us with a scope of comparative analysis of the GNSS scintillation over Waltair. The observations are segregated on basis of occurrence and strength of scintillation for dependence on frequency, visible and scintillation-affected satellites, time window and seasons besides monthly percentage statistics, thus making this study a highly quantitative comparison of the phenomena. It can be noted that the equinox and solstice specific dates are marked in Figs. 1–5 along the variation in solar activity to bring forth the seasonal response of scintillations in

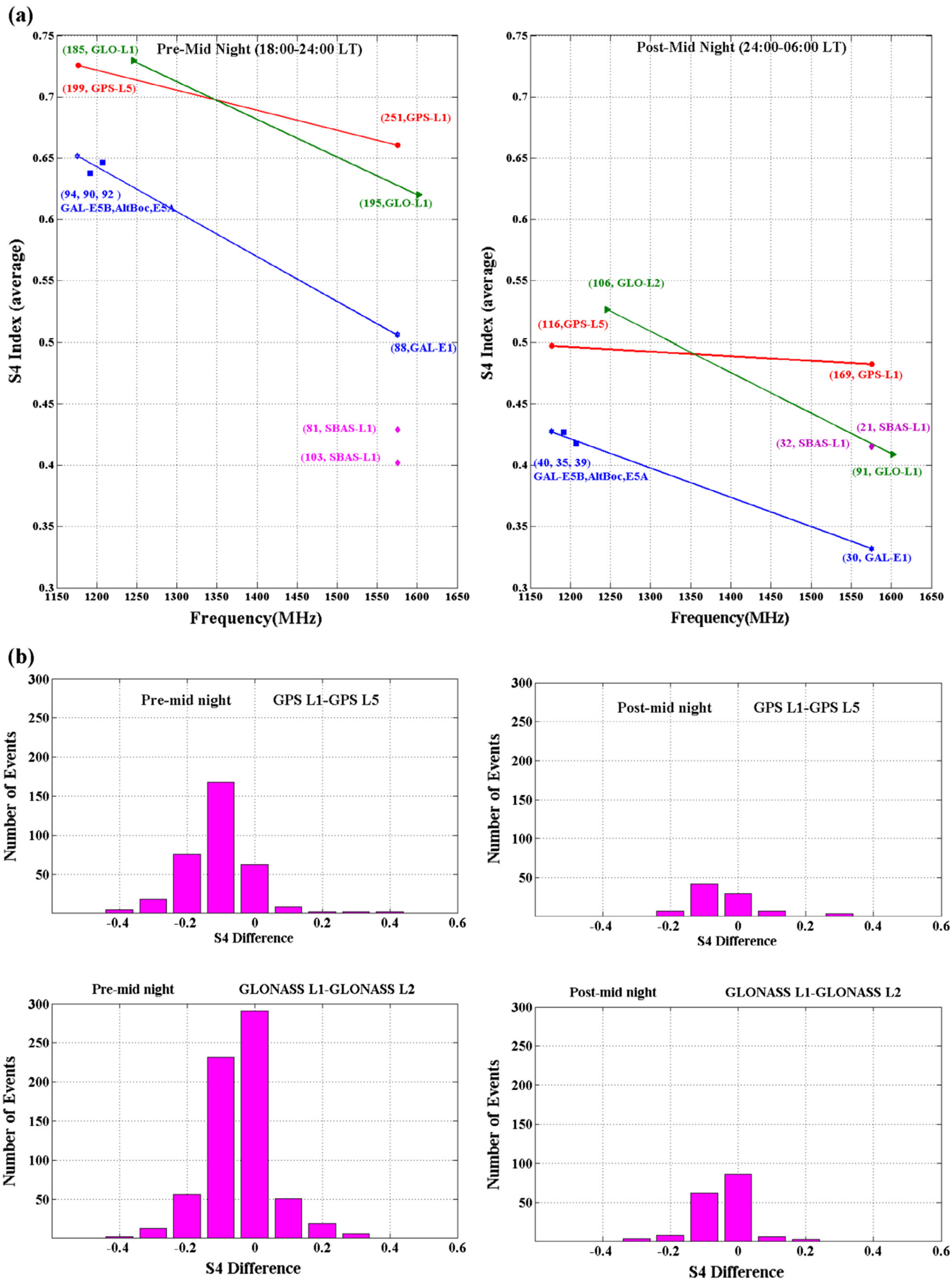

Fig. 6. (a) Gross averages of all peak S4 indices obtained from all the visible satellites in the 6 h time window for a given GNSS constellation from all observations in left panel (pre-midnight) and right panel (post-midnight) time windows. (b) Difference in mean S4 magnitude between GPS L1 and L5 (top panels) and GLONASS L1 and L2 bands (bottom panels).

backdrop of changing solar activity in all the above categories of observations.

3.1. General observations

As noted above, Fig. 1a and b present per minute peak S4 for all the GNSS observations. The first panel of Fig. 1a shows the maximum scintillation occurrence in equinoctial months followed by winter and summer months during the concerned period of observations. It is obvious that there exists a decreasing trend in scintillation occurrence with seasonal highs (around equinoxes) and lows (around solstices). The occurrence of scintillations is mostly dominant between 19:00–02:00 IST, however, the scintillation is observed up to 03:00 IST for a very few events. Also it is noteworthy that the occurrence of scintillations is more severe around the March equinox of 2015 than any other seasons in the whole concerned period. As far as the occurrence of scintillation among different frequencies is concerned, the GPS L1 frequency shows highest occurrence and temporal width whereas GPS L5 show highest strength of scintillation compared to other frequencies of GLONASS, SBAS and Galileo in L1 band. Similar results are obtained in Fig. 1b for different frequencies in L2 and other bands. Table 1 shows that each of the frequency is sensitive to a particular Fresnel scale of irregularities ranging from 361 m to 422 m for all the GNSS signals. Hence a direct comparison is not warranted because theoretically, the Fresnel scales not too widely spaced to get affected by scintillation in so drastically different manner. Also it is intriguing to note that E1 and E5 frequencies of Galileo show the weakest and least occurrences, whereas L1 of SBAS remains lesser in all respect than L1 and L2 of GLONASS. Such a conclusive and direct comparison remains incomplete from the present study with due knowledge that various constellations have different number of satellites and visibility over a site. Thus, with a bird's eye view of general observations presented in Fig. 1a and b, the comparative analyses of the occurrence and strength of S4 call to account for the availability of satellites and number of satellite passes affected by S4. This analysis, which is uniquely performed in this study, is detailed below.

3.2. Satellite visibility and frequency dependence of S4

Fig. 2a and b emphasize this aspect of aimed comparison between different frequencies and constellations in pre-midnight and post-midnight periods. The results of Fig. 2a and b clearly show the peak S4 on a particular frequency in respective durations of 6 h per night over Waltair irrespective of specific satellite of a system. These figures show the severity of scintillation and its daily variation for different frequencies. It is obvious that a reasonable agreement exists among the frequencies for the peak value of S4 index as given in each panel of Fig. 2a and b. The closely spaced bars in these figures indicate the higher daily occurrence. Evidently, the occurrence of scintillation for GPS and GLONASS in both pre and post-midnight windows remain higher than Galileo and SBAS satellites (see Table 2 for details on number of available satellites). It is well known the EPBs are formed in the equatorial ionosphere, preferably, in the post-sunset sector, through nonlinear Rayleigh-Taylor instability process in conducive background conditions on a given night (Haerendel, 1973; Woodman and La Hoz, 1976; Zalesak and Ossakow, 1980, etc.). A detailed treatise of scientific literature on various aspects of EPBs is provided by Kelley (2009). The variability in the triggering, evolution, drift and decay characteristics of this plasma instability have well been reported from various longitude sectors e.g. Fejer et al. (1999), Fritts et al., (2009), Tsunoda (2010), Yokoyama et al. (2011) and references therein. The theoretical framework for ionospheric scintillations associated with EPBs is well founded by Yeh and Liu (1982), Bhattacharyya et al. (1992), Wernik et al. (2003) and Rino (2011) and the observational evidences of the variability in GPS scintillations due to EPBs are reported from around the globe e.g. Groves et al. (1997), Dashora and Pandey, (2005), Rama Rao et al. (2006) and Paznukhov et al. (2012) and many previous studies. In view of the present understanding of this phenomena, the above mentioned results from Figs. 1 and 2 highlight the contrast among the various GNSS systems for scintillation occurrence as well as strength. This signifies spatial as well as temporal variability of the EPBs in the coverage area above

Table 2
Duration of data records over Waltair and number of available satellite in pre and post midnight time windows.

GNSS system Data available Over Waltair		GPS July 2014–August 2016		GLONASS November 2014–August 2016		Galileo November 2014–August 2016				Indian SBAS May 2015–August 2016
Frequency		L1	L5	L1 Band	L2 Band	E1	E5A	E5B	AltBOC	L1
Pre mid night	Max. available	16	8	11	11	6	6	6	6	2
	Avg. available	13	4	9	9	3	3	3	2	2
	Max. affected	12	7	9	9	4	4	4	4	2
No. of PRNs										
Post mid night	Max. available	16	7	11	11	6	6	6	5	2
	Avg. available	13	4	9	9	3	3	3	2	2
	Max. affected	16	6	7	8	3	3	3	3	2
No. of PRNs										

Waltair and the associated scintillation for a given satellite system for time interval of 6 h. In fact, Fig. 3a and b illustrates this contrast further in terms of visible and affected number of satellites over Waltair. The first interesting fact to note is that number of visible satellites transmitting GPS L5 signal are significantly less (by one third) than that transmitting GPS L1 for a given time window on a given night. Also the number of visible satellites in GPS L5 frequency shows an annual variability peaking around winters for pre-midnight and around September equinoxes in post-midnight windows. Nevertheless, as mentioned above, Fig. 2a and b showed similar pattern in terms of the peak S4 and daily occurrence for GPS L1, GPS L5 and GLONASS L1 and L2 band of frequencies. This leads to a new result that the magnitude of the peak S4 over Waltair remains independent of frequency, satellite and the system for a given night as far as GPS and GLONASS are concerned. Whereas the lesser number of visible satellites in Galileo and constant number of visible satellite in SBAS produce a less populated daily occurrence pattern with comparable peak S4 to GPS and GLONASS (Fig. 2a and b). The availability of Galileo satellites up to January 2016 remained very low (Fig. 3a and b), and the satellite passes visible within the elevation cutoff remained limited to a few minutes for each pass occupying less coverage area. Whereas, both the SBAS satellites have been continuously visible but they exhibit a daily occurrence pattern (Fig. 2a and b) similar to the Galileo satellites in the respective time windows. In nutshell, the daily occurrence and the peak magnitude of scintillation partly seems to be frequency and system independent. This illustrates that on a given night, when EPBs occur over Waltair, the peak S4 in a large volume over this site in a time window of 6 h exhibit frequency independence. Also it is noted that the percentage of visible satellites affected by scintillation shows a frequency and system dependence (discussed in later sections).

3.3. Seasonal, pre- and post-midnight dependence

Monthly percentage occurrence of scintillation for the two time windows is respectively shown in Fig. 4a and b. The occurrence data from Fig. 1a and b has been used to prepare this result for both the time windows. It is obvious from Fig. 4a that the percentage occurrence exhibit maximum for March equinoxes (February, March, April months) followed by September equinoxes (August, September, October months), winters (November, December, January months) and summers (May, June, July months). There are a few interesting observations in this figure for example, the occurrence in the months of August (i.e. equinoctial period) are less compared to the months of November (winters) and no scintillation is observed in the months of May and June 2016 except for SBAS PRN 127. Besides it can be noted that highest occurrence for GPS L1 is as large as about 80% in April 2015 and least in July 2015 and July-August of 2016 (top left (i) panel of Fig. 4a). The highest percentage occurrence for GPS L5 is about 68% in February–March 2015 and the least in the summer months of 2015 and 2016 (Fig. 4a–vi). It is evident that GPS L1 and L5 occurrences are largely controlled by the number of signals transmitted by the satellites in view, which is very small for L5 frequency in this time window. The (ii) and the (vii) panels of Fig. 4a show percentage occurrence for GLONASS L1 and L2 bands respectively and the highest scintillation activity of about 68% is observed in March 2015 in both the frequency bands. The summer months of 2016 show no scintillation activity for L2 band of GLONASS. The Galileo signal in bands of E1, E5A, E5B, AltBOC and SBAS PRN 127 and 128 signals (in L1) show the highest scintillation activity in March 2016 with 42%, 49%, 48%, 46%, 55% and 55% respectively and no scintillation is observed in the month of July 2015. The SBAS PRN128 showed no scintillation activity in May 2016 in addition to aforementioned occurrence pattern.

Thus, the results show a strong seasonal character in percentage occurrence pattern as has been reported in many previous studies for VHF and L-bands (Aarons, 1993; Basu et al., 1988; Paznukhov et al., 2012; Akala et al., 2016). The largely accepted mechanism for equinox (high) and solstice (low) climatology is given by Tsunoda (1985) illustrating the alignment of local geomagnetic field line with evening solar terminator that affect the seeding and growth of EPBs (Fejer et al., 1999; Tsunoda, 2010). While, grossly, the results of this study follow this climatology, but from a GNSS user point of view, the climatology differs in various regards to the previous studies for example it is found that the seasonal pattern largely differs from one frequency to another and same is true for different GNSS systems (see Groves et al., 1997 and the aim of SCINDA network). In this regard, the difference of climatology between GPS L1 and L5 is significant due to visibility but the difference is insignificant between GLONASS L1 and L2 bands due to similar visibility over Waltair. Thus, it is not only the frequency but also the number of satellites in a given system transmitting a particular signal that plays a major role in defining percentage occurrence over a site. In view of work by Wiens et al. (2006) that the scintillations in L-band in later hours of evening are affected by evolving and drifting EPBs and depend largely on the background conditions from night to night in a given season, a large variability is not unexpected. But, in addition to such large variability in occurrence of EPBs and their relation with L-band scintillation, our results exhibit further complexity to apprehend the kind of GNSS system, number of available satellites and frequency used by the GNSS system.

In fact novel results as shown in Fig. 4b for the post-midnight window are significant due to the fact that a large percentage occurrence is noted in GPS and GLONASS observations compared to other systems. It is also interesting to note that the peak seasonal occurrence is observed in September equinoxes for GPS L1 and L5 compared to March equinoxes. This result is reverse of the occurrence pattern as observed in pre-midnight window, specifically applicable for GPS signals. In case of pre-midnight occurrence, the peak percentage occurrence as well as the seasonal pattern showed almost similar values. The post-midnight occurrence in case of solstices is seen to be favored more by winter background than summer. Specifically, the May, June and July months of summer have shown negligible scintillations during post-midnight.

3.4. Strength of scintillation and affected satellites passes

The statistical analysis presented in Fig. 4a and b was aimed to count the number of days irrespective of affected satellites and the strength of scintillation. Thus, to estimate the magnitude of scintillation over the different GNSS signals and to find the affected number of satellite passes, the S4 data is segregated in three categories of weak, moderate and strong scintillations as mentioned in Section 2. The results for the two time windows are presented in Fig. 5a and b, respectively for pre-midnight and post-midnight periods. The abscissa of the columnar panels of the figures show the number of satellite passes having scintillations in three categories (mentioned above) for a given month and the ordinate show the month of the year. On top of each panel in both the Fig. 5a and b, the highest percentage occurrence of affected satellite passes for each category found in a specific month is given. It can be seen from the Fig. 5a (pre-midnight window) that the magnitude of S4 over GPS L1frequency show highest number of passes with strong scintillation occurring in April 2015 (138 out of 178 passes); with moderate scintillations occurring in February 2015 (29 passes out of 67) and with weak scintillations occurring in January 2016 (25 out of 46). Similarly, the other panels of Fig. 5a show that the strong scintillations occur in majority of passes during equinoxes over all frequencies, however, the solstice seasons generally show higher number of passes with weak and moderate scintillations compared to the strong scintillations. A very noteworthy feature that can be clearly seen from Fig. 5a is effect of decreasing solar activity on the magnitude of the scintillations in the three categories over different frequencies.

The first feature is that the total number occurrence of S4 over GPS and GLONASS frequencies has reduced by about half after August 2015 compared to before it. However, there is an increase in number occurrence for Galileo signals in 2016 which is directly correlated with increase of number satellites after January 2016 (refer to Fig. 3a and b for number of visible satellites). The second feature is that the solar activity related decrement has occurred only for the strong scintillations whereas the decrement in solar activity has resulted in increase in number of passes having weak or moderate scintillations and that has occurred only for GPS and GLONASS signals. When comparing the magnitude of S4 between GLONASS L1 and L2 bands, it is found that L2 band shows higher total number of passes with more weak and moderate scintillations than on L1 band after August 2015 compared to before it. So, it seems that strength of scintillations show a frequency dependence that reverses when solar activity is declining. Thus, for higher solar activity, the scintillations in L1 band dominate with more number of strong cases but for decreasing solar activity, the scintillations in L2 band dominate with more weak and moderate cases. To the best of our knowledge, we believe that such a result has not been reported so far and makes a case of novelty from this work. As far as variations in magnitude of S4 for GPS L5 is concerned, it needs to be seen in light of visibility when comparing it with GPS L1. As noted above, that there is a concern of visibility for Galileo satellites which increased after January 2016 so a direct effect of solar activity on the magnitude and satellite passes cannot be gauged. Another interesting statistics that is estimated from Fig. 5a is the highest number of passes affected by each category of scintillation out of all months indicated above the top of each of the panels. According to the maximum visibility (from Fig. 3a and b) the GPS L1 and GLONASS L1 and L2 bands could provide a reasonable estimate of the statistics of passes affected by scintillation. Thus, including the results from GPS L1 and GLONASS L1 and L2 results to arrive at this percentage, it is found that in the pre-midnight window, the peak number of passes affected by strong, moderate and weak scintillations range from 69% to 87%, from 21% to 27% and from 36% to 54%, respectively. In nutshell, the results show significant effects of strong, moderate and weak scintillations on GNSS signals in Indian zone.

Coming to the case of post-midnight scintillations as shown in Fig. 5b, it is found that the scenario changes drastically both in terms of magnitude and number occurrence of affected satellite passes. The effect of decrease in solar activity has resulted in an overall decrement in post midnight scintillation after August 2015 by three times than before. However, in case of pre-midnight scintillations, the decrement after August 2015 is less observed than before. For GPS L1 and GLONASS L1 and L2, it is found that in the post-midnight window, the peak number of passes affected by strong, moderate and weak scintillations range from 31% to 60%, from 25% to 59% and from 30% to 55%, respectively. Thus, a very important aspect coming out of this study is the presence of majority of moderate and weak scintillations in post-midnight compared to majority of strong scintillations in case of pre-midnight window. The seasonal pattern remains almost comparable to the pre-midnight case, albeit with very low number occurrence. Very intriguingly, the summer solstices do not exhibit higher number occurrence during post-midnight window at any level of solar activity, in contrast to previous studies for VHF scintillations. Thus in post-midnight window, a drastic difference noted above remains a puzzle to explain during low solar activity periods as also has been reported by Yokoyama et al. (2011) using C/NOFS observations during 2008–2009. It has remained a recent scientific quest centered about two particular hypotheses, the first one belongs to identifying suitable source mechanisms that could sustain the EPBs in post-midnight (Patra et al., 2009) and second belongs to identifying the source within EPB that could produce 300–400 m-scale irregularities and cause L-band scintillations in this period. While fresh generation of EPBs in midnight local longitude sector is so far not implied in most theories but MSTID (medium scale traveling ionospheric disturbance) are found to be a plausible answer behind meter-scale radar backscatter in post-midnight (Otsuka et al., 2009) during declining and low solar activity periods. With regard to GPS scintillations, recently Abadi et al. (2014) presented post-midnight observation from rising phase of solar activity with an elevation cut-off of 30°. However, our observations are from declining and low solar activity period and report probably the first longest term continuous activity in post-midnight with decreasing solar activity. Moreover, present results show a peak in September (equinox) rather than summer period in contrast to previous radar observations. The low solar activity and its impact on nocturnal ionosphere have been studied for the last solar cycle 23 in various studies as referred in Sections 1 and 3 above. The most peculiar question is on intriguing occurrence of post-midnight L-band scintillation as solar activity tends towards minima. The cause probably lies either in the drifting EPBs that are not fossil bubbles and could sustain the 300 m scale irregularities or the equatorward traveling MSTIDs that scatter the GNSS signals in peculiar fashion as seen in radar observations (Patra et al., 2009) to cause weak/moderate scintillations. It is planned to take a coordinated study to understand the phenomena in upcoming solar minima of cycle 24.

3.5. Frequency dependence of mean S4

As noted above, the simultaneous availability of S4 measurements over all GNSS signals provide an opportunity to derive a relation between mean S4 and different frequencies. Fig. 6 presents the plots of average of all peak S4 indices obtained from all the visible satellites in the 6 h time window for a given constellation from all observations.

The red line shows the results from GPS, green for GLONASS and blue for Galileo signals respectively for pre-mid night (left panel) and post-mid night (right panel) windows. The number given in brackets near each square marker on the lines show the number of nights for which the peak of S4 is averaged for that frequency of signal. An obvious appearance of negative slope for all three lines in both time windows illustrates the mean dependence of S4 on frequency. The negative slopes for GPS, GLONASS and Galileo frequencies are 0.16, 0.31 and 0.37 per GHz for pre-mid night and are 0.03, 0.33 and 0.24 per GHz for the post-mid night time windows. The slope for GPS and Galileo may be affected by the simultaneous visibility of satellites transmitting the concerned signals. Also an obvious difference between the pre-mid night and post-mid night S4 variations for each GNSS system is visible in terms of mean value of S4 for a given frequency. Additionally, this fact is quantified in Fig. 6b which shows the number of events with regard to difference in mean S4 magnitude between GPS L1 and L5 (top panels) and GLONASS L1 and L2 bands (bottom panels). Clearly, the more number of events showing negative difference indicate that most of the time the S4 remains larger on lower frequency L2 than L1. Theoretically, the variations in S4 index are inversely proportional to square of the frequency (Bhattacharyya et al., 1992), but on average not all signals/satellites show such relation in this study; besides on average S4 is inversely proportional to the frequency of the signal even at mean of several such cases. Also it shall be noted that each system show a remarkable difference with other systems/signals for the similar cases and it highlights the issues of tracking multiple GNSS signals in a receiver and future GNSS users at large because each system would require addressing scintillations separately.

4. Summary

This study reveals a few new and unique features of multi-frequency multi-GNSS scintillations by using, so far, the longest and continuous data records from the solar cycle 24. Waltair is located at the crest of ionization anomaly in Indian sector and hence the results are also the first of this kind from India from such a geophysical location of importance for scintillation studies. A robust comparative analysis of effect of ionospheric irregularities on different frequencies of various satellite navigation systems is performed. The results are presented from point of views of scientific quest as well as effects of ionosphere on the GNSS applications. The quantitative analysis uniquely reveals that apart from the solar cycle and seasonal effects, the number of visible satellites of a selected GNSS markedly affect the occurrence and also the strength. The strength and occurrence of strong scintillations decrease with declining solar activity during pre-midnight hours but remarkably increase for moderate and weak scintillations during post-midnight. Finally, inter-GNSS signal analysis in terms of the effect of strong, moderate and weak scintillations is presented with due consideration of number of satellite passes affected and frequency dependence of mean S4. The results of this study are valuable considering the scope of GNSS applications that require precise positioning with integrity in various domains. Particularly, from point of view of scintillations in equatorial zones, the performance of a GNSS receiver is affected when the code and carrier phase tracking loops lose the lock on the incoming signals. The results of this study emphasize for the first time the effects of low latitude scintillation on different types of GNSS signals in Indian zone under changing background conditions. In future we aim to study the effect of equatorial scintillations on the events of loss of lock under various background conditions in quiet as well as space weather events with varying levels of solar activity.

Acknowledgements

Authors express sincere thanks to ISRO (Indian Space Research Organization) for providing GPStation-6 under SSPS (Space Science Promotion Scheme) program. VKD Srinivasu acknowledges the BSR (Basic Scientific Research) junior research fellowship provided by UGC (University Grants Commission), India. Thanks are due to the Director, NARL (National Atmospheric Research Laboratory) for supporting this collaborative work.

References

Aarons, J., 1982. Global morphology of ionospheric scintillations. Proc. IEEE 70 (4), 360–378.

Aarons, J., 1993. The longitudinal morphology of equatorial F layer irregularities relevant to their occurrence. Space Sci. Rev. 63, 209–243. https://doi.org/10.1007/BF00750769.

Abadi, P., Saito, S., Srigutomo, W., 2014. Low-latitude scintillation occurrences around the equatorial anomaly crest over Indonesia. Ann. Geophys. 32, 7–17. https://doi.org/10.5194/angeo-32-7-2014.

Akala, A.O., Awoyele, A., Doherty, P.H., 2016. Statistics of GNSS amplitude scintillation occurrences over Dakar, Senegal, at varying elevation angles during the maximum phase of solar cycle 24. Space Weather 14, 233–246. https://doi.org/10.1002/2015SW001261.

Basu, S., MacKenzie, E., Basu, S., 1988. Ionospheric constraints on VHF/UHF communications links during solar maximum and minimum periods. Radio Sci. 23 (3), 363–378. https://doi.org/10.1029/RS023i003p00363.

Basu, S., Basu, Su., 1981. Equatorial scintillation—a review. J. Atmos. Terr. Phys. 43, 473–489. https://doi.org/10.1016/0021-9169(81)90110-0.

Basu, S., Groves, K.M., Quinna, J.M., Doherty, P., 1999. A comparison of TEC fluctuations and scintillations at Ascension Island. J. Atmos. Sol.-Terr. Phys. 61 (16), 1219–1226.

Bhattacharyya, A., Yeh, K.C., Franke, S.J., 1992. Deducing turbulence parameters from transionospheric scintillation measurements. Space Sci. Rev. 61 (3–4), 335–386. https://doi.org/10.1007/BF00222311.

Briggs, B.H., Parkins, I.A., 1963. On the variation of radio star and satellite scintillations with zenith angle. J. Atmos. Terr. Phys. 25, 339–365.

Carrano, C.S., Groves, K.M., 2010. Temporal decorrelation of GPS satellite signals due to multiple scattering from ionospheric irregularities. In: Proceedings of the 23rd International Technical Meeting of the Satellite Division of the Institute of Navigation (ION GNSS 2010), Portland, OR, September 2010, pp. 361–374.

Carrano, C.S., Groves, K.M., McNeil, W.J., Doherty, P.H., 2012. Scintillation characteristics across the GPS frequency band. In: Proceedings of the 25th International Technical Meeting of the Satellite Division of the Institute of Navigation (ION GNSS 2012), Nashville, Tenn, pp. 1972–1989.

Chakraborty, S.K., Chatterjee, S., Das Gupta, A., 2014. SBAS operation in the Indian sector under simultaneous scintillation on different GNSS links. J. Atmos. Sol.-Terr. Phys., 50–57 https://doi.org/10.1016/j.jastp.2014.04.005.

Conker, R.S., El Arini, M.B., Hegarty, C.J., Hsiao, T., 2003. Modeling the effects of ionospheric scintillation on GPS/SBAS availability. Radio Sci. 38, 1–23. https://doi.org/10.1029/2000RS002604.

Das Gupta, A., Rat, S., Paul, A., Banerjee, P., Bose, A., 2004. Errors in position-fixing by GPS in an environment of strong equatorial scintillations in the Indian zone. Radio Sci. 39 (RS1S30). https://doi.org/10.1029/ 2002RS002822.

Dashora, N., Pandey, R., 2005. Observations in equatorial anomaly region of total electron content enhancements and depletions. Ann. Geophys. 23 (7), 2449–2456. https://doi.org/10.5194/angeo-23-2449-2005.

Dashora, N., Suresh, S., 2015. Characteristics of low-latitude TEC during solar cycles 23 and 24 using global ionospheric maps (GIMs) over Indian sector. J. Geophys. Res. Space Phys. 120, 5176–5193. https://doi.org/10.1002/2014JA020559.

Fejer, B.G., Scherliess, L., de Paula, E.R., 1999. Effects of vertical plasma drift velocity on the generation and evolution of equatorial spread F. J. Geophys. Res. 104, 19 859–19 869.

Fritts, D.C., Abdu, M.A., Batista, B.R., Batista, I.S., Batista, P.P., Buriti, R., Clemesha, B.R., Dautermann, T., de Paula, E.R., Fechine, B.J., Fejer, B.G., Gobbi, D., Haase, J., Kamalabadi, F., Kherani, E.A., Laughman, B., Lima, P.P., Liu, H.-L., Medeiros, A., Pautet, P.-D., Riggin, D.M., Rodrigues, F.S., São Sabbas, F., Sobral, J.H.A., Stamus, P., Takahashi, H., Taylor, M.J., Vadas, S.L., Vargas, F., Wrasse, C.M.Overview and summary of the Spread F Experiment (SpreadFEx), 2009. Ann. Geophys. 27, 2141–2155. https://doi.org/10.5194/angeo-27-2141-2009.

Ghafoori, F., Skone, S., 2015. Impact of equatorial ionospheric irregularities on GNSS receivers using real and synthetic scintillation signals. Radio Sci. 50, 294–317. https://doi.org/10.1002/2014RS005513.

GPStation-6™, 2012. GNSS Ionospheric Scintillation and TEC Monitor (GISTM) Receiver. User Manual, OM-20000132, Rev 2, November 2012, NovAtel Inc., Calgary, Canada.

Groves, K., Basu, S., Weber, E., Smitham, M., Kuenzler, H., Valladares, C., Sheehan, R., MacKenzie, E., Secan, J., Ning, P., McNeil, W., Moonan, D., Kendra, M., 1997. Equatorial scintillation and systems support. Radio Sci. 32, 2047–2064.

Haerendel, G., 1973. Theory of Equatorial Spread-F, Report, Max-Planck-Inst. ftir Extraterr. Phys., Garching bei Munchen, Germany.

Hlubek, N., Berdermann, J., Wilken, V., Gewies, S., Jakowski, N., Wassaie, M., Damtie, B., 2014. Scintillations of the GPS, GLONASS, and Galileo signals at equatorial latitude. J. Space Weather Space Clim. 4, A22. https://doi.org/10.1051/swsc/2014020.

Hofmann-Wellenhof, B., Lichtenegger, H., Wasle, E., 2008. GNSS—Global Navigation Satellite Systems: GPS, GLONASS, Galileo, and More. Springer-Verlag Wien, Vienna, Austria, ISBN 978-3-211-73012-6, doi:10.1007/978-3-211-73017-1..

Kelley, M.C., 2009. The Earth's Ionosphere: plasma physics and electrodynamics. In: International Geophysics Series, vol. 43. Academic Press, San Diego, USA. http://dx.doi.org/10.1126/science.248.4951.89.

Kintner, P.M., Kil, H., Beach, T.L., dePaula, E.R., 2001. Fading timescales associated with GPS signals and potential consequences. Radio Sci. 36 (4), 731–743. https://doi.org/10.1029/1999RS002310.

McClure, J.P., Hanson, W.B., Hoffman, J.H., 1977. Plasma bubbles and irregularities in equatorial ionosphere. J. Geophys. Res. 82, 2650–2656. https://doi.org/10.1029/JA082i019p02650.

Muella, M.T.A.H., de Paula, E.R., Kantor, I.J., Rezende, L.F.C., Smorigo, P.F., 2009. Occurrence and zonal drifts of small-scale ionospheric irregularities over an equatorial station during solar maximum – magnetic quiet and disturbed conditions. Adv. Space Res. 43, 1957–1973. https://doi.org/10.1016/j.asr.2009.03.017.

Otsuka, Y., Shiokawa, K., Ogawa, T., 2006. Equatorial ionospheric scintillations and zonal irregularity drifts observed with closely spaced GPS receivers in Indonesia. J. Meteorol. Soc. Jpn. 84A, 343–351.

Otsuka, Y., Ogawa, T., Effendy, 2009. VHF radar observations of nighttime F-region field-aligned irregularities over Kototabang, Indonesia. Earth Planets Space 61, 431–437. https://doi.org/10.1186/BF03353159.

Patra, A.K., Phanikumar, D.V., Pant, T.K., 2009. Gadanki radar observations of F region field-aligned irregularities during June solstice of solar minimum: first results and preliminary analysis. J. Geophys. Res. 114, A12305. https://doi.org/10.1029/2009JA014437.

Paznukhov, V.V., Carrano, C.S., Doherty, P.H., Groves, K.M., Caton, R. G., Valladares, C.E., Seemala, G.K., Bridgwood, C.T., Adeniyi, J., Amaeshi, L.L.N., Damtie, B., DUjanga, F.M., Ndeda, J.O.H., Baki, P., Obrou, O.K., Okere, B., Tsidu, G.M., 2012. Equatorial plasma bubbles and L-band scintillations in Africa during solar minimum. Ann. Geophys. 30, 675–682. https://doi.org/10.5194/angeo-30-675-2012.

Rama Rao, P.V.S., Gopi Krishna, S., Niranjan, K., Prasad, D.S.V.V.D., 2006. Study of spatial and temporal characteristics of L-band scintillations over the Indian low-latitude region and their possible effects on GPS navigation. Ann. Geophys. 24, 1567–1580, www.ann-geophys.net/24/1567/2006/.

Rama Rao, P.V.S., Gopi Krishna, S., Prasad, S.N.V.S., Prasad, D.S.V.V.D., Niranjan, K., 2009. Geomagnetic storm effects on GPS based navigation. Ann. Geophys. 27 (5), 2101–2110. https://doi.org/10.5194/angeo-27-2101-2009.

Rino, C., 2011. The Theory of Scintillation with Applications in Remote Sensing. Wiley-IEEE Press, ISBN: 978-0-470-64477-5.

Secan, J.A., Bussey, R.M., Fremouw, E.J., Basu, S., 1995. An improved model of equatorial scintillation. Radio Sci. 30 (3), 607–617. https://doi.org/10.1029/94RS03172.

Spogli, L., Alfonsi, L., Romano, V., De Franceschi, G., Francisco, J., Monico, G., Shimabukuro, M.H., Bougard, B., Aquino, M., 2013. Assessing the GNSS scintillation climate over Brazil under increasing solar activity. J. Atmos. Terr. Phys. 105–106, 199–206. https://doi.org/10.1016/j.jastp.2013.10.003.

Tsunoda, R.T., Livingston, R.C., McLure, J.P., Hanson, W.B., 1982. Equatorial plasma bubbles: vertically elongated wedges from the bottom side F layer. J. Geophys. Res. 87, 9171–9180.

Tsunoda, R.T., 1980. Magnetic field aligned characteristics of plasma bubbles in the night time ionosphere. J. Atmos. Terr. Phys. 42, 743–752.

Tsunoda, R.T., 1985. Control of the seasonal and longitudinal occurrence of equatorial scintillations by the longitudinal gradient in integrated E region Pedersen conductivity. J. Geophys. Res. 90, 447–456. https://doi.org/10.1029/JA090iA01p00447.

Tsunoda, R.T., 2010. On seeding equatorial spread F during solstices. Geophys. Res. Lett. 37, L05102. https://doi.org/10.1029/2010GL042576.

Valladares, C.E., Villalobos, J., Sheehan, R., Hagan, M.P., 2004. Latitudinal extension of low-latitude scintillations measured with a network of GPS receivers. Ann. Geophys. 22, 3155–3175. https://doi.org/10.5194/angeo-22-3155-2004.

Venkatesh, K., Rama Rao, P.V.S., Seemala, G.K., Prasad, D.S.V.V.D., 2015. Latitudinal variation in the occurrence of GPS L-band scintillations associated with the day-to-day changes in TEC, h′ F and the E × B drift velocity and their impact on GPS satellite signals. J. Earth Syst. Sci. 124 (3), 497–513. https://doi.org/10.1007/s12040-015-0558-9.

Wernik, A.W., Secan, J.A., Fremouw, E.J., 2003. Ionospheric irregularities and scintillation. Adv. Space Res. 31 (4), 971–981. https://doi.org/10.1016/S0273-1177(02)00795-0.

Whitney, H.E., 1974. Notes on the Relationship of Scintillation Index to Probability Distribution and Their Uses for System Design. Rep. AFCRL-TR-74-0004, Air Force Cambridge Res. Lab., Hanscom Air Force Base, Massachusetts, USA.

Wiens, R.H., Ledvina, B.M., Kintner, P.M., Afewerki, M., Mulugheta, Z., 2006. Equatorial plasma bubbles in the ionosphere over Eritrea: occurrence and drift speed. Ann. Geophys. 24, 1443–1453. https://doi.org/10.5194/angeo-24-1443-2006.

Woodman, R.F., La Hoz, C., 1976. Radar observations of F region equatorial irregularities. J. Geophys. Res. 81, 5447–5466. https://doi.org/10.1029/JA081i031p05447.

Yeh, C.K., Liu, C.H., 1982. Radio wave scintillations in the ionosphere. Proc. IEEE 70 (4), 324–360.

Yokoyama, T., Yamamoto, M., Otsuka, Y., Nishioka, M., Tsugawa, T., Watanabe, S., Pfaff, R.F., 2011. On post-midnight low-latitude ionospheric irregularities during solar minimum: 1. Equatorial atmosphere radar and GPS-TEC observations in Indonesia. J. Geophys. Res. 116, A11325. https://doi.org/10.1029/2011JA016797.

Zalesak, S.T., Ossakow, S.L., 1980. Nonlinear equatorial spread F: spatially large bubbles resulting from large horizontal scale initial perturbations. J. Geophys. Res. 85, 2113–2142.